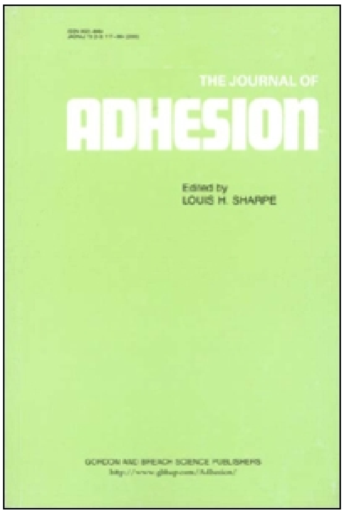

The Journal of Adhesion

The Effects of Cure Temperature and Time on the Stress-Whitening Behavior of Structural Adhesives. Part II. Analysis of Fractographic Data

Hooshang Jozavi[a]; Erol Sancaktar[a]
[a] Department of Mechanical and Industrial Engineering, Clarkson University, Potsdam, New York, U.S.A.

To cite this Article Jozavi, Hooshang and Sancaktar, Erol(1989) 'The Effects of Cure Temperature and Time on the Stress-Whitening Behavior of Structural Adhesives. Part II. Analysis of Fractographic Data', The Journal of Adhesion, 27: 3, 159 — 174

To link to this Article: DOI: 10.1080/00218468908048450

URL: http://dx.doi.org/10.1080/00218468908048450

J. Adhesion, 1989, Vol. 27, pp. 159–174
Reprints available directly from the publisher
Photocopying permitted by license only

The Effects of Cure Temperature and Time on the Stress-Whitening Behavior of Structural Adhesives. Part II. Analysis of Fractographic Data

HOOSHANG JOZAVI and EROL SANCAKTAR

Department of Mechanical and Industrial Engineering, Clarkson University, Potsdam, New York 13676, U.S.A.

(Received November 21, 1987; in final form September 9, 1988)

In this second part of the paper on the effects of cure conditions on the stress-whitening behavior of structural adhesives, fractographic data are presented and discussed. For this purpose, the size and nature of crack-tip-whitening zones obtained using single edge notched tension specimens of the model adhesive Metlbond with and without carrier cloth are studied. Scanning electron photomicrographs are utilized to investigate the effects of cure temperature and time on the crack-tip stress-whitening behavior. A brief discussion on the formation of inherent voids during the cure process is also presented since they are observed to enhance the crack-tip-whitening zones. Experimental results reveal that both the extent of voids produced during the cure process and the size of the crack-tip-whitening zones on the fracture surface increase with increasing cure temperatures. The presence of carrier cloth produces a similar effect with increases in both inherent voiding and stress-whitening sizes. The creation of stress-whitening zones are linked to stable crack propagation in those areas.

KEY WORDS Stress-whitening zone; crack tip plastic deformation; stable and catastrophic crack propagation; effects of cure temperature and time; effects of carrier cloth; formation and effects of inherent voids.

INTRODUCTION

In Part I of this paper an analytical method of defining and calculating stress-whitening stress σ^* and strain ε^* values was reviewed. The analytical method consisted of a modified bilinear form of the Ramberg–Osgood equation (RAMOD-2) which was used in conjunction with bulk tensile data. The cure conditions: temperature, time and cool-down rate were shown to affect, considerably, the Ramberg–Osgood exponent n_1 and the stress-whitening parameters σ^* and $1/n_2$. It was pointed out that the fracture toughness K_{IC} and the parameter $1/n_2$ exhibited similar behaviors as they both decreased with increasing cure temperature.[1]

The tensile strength (σ_y), stress-whitening stress (σ^*) and the parameter $1/n_1$ were also shown to exhibit similar behaviors with respect to the cure temperature. These parameters first increased up to a peak and then decreased as the cure temperature was increased. The peak (optimum) value for all three parameters were shown to lie somewhere between 99°C and 110°C with good correlation to the Tg (~112°C) of the model adhesive Metlbond 1113.

The use of a slow cool-down condition was shown to result in higher σ^*, $1/n_1$ and $1/n_2$ values, which indicated higher resistance to fracture.

Fracture data obtained using Single Edge Notched (SEN) tension specimens of the same model adhesive Metlbond with (1113) and without (1113-2) carrier cloth will be analyzed in this paper in relation to stress whitening at the crack tip. For this purpose, scanning electron photomicrographs will be utilized and the effects of cure temperature and time on the crack tip stress-whitening behavior will be investigated.

A brief discussion on the formation of voids during the cure process will also be presented since they are observed to enhance the crack tip whitening zones.

As discussed previously, the cure-history-dependent stress whitening that takes place during the deformation and fracture of the model adhesives both in bulk tensile and fracture specimens is an important feature of these materials. The model adhesives used in this work are rubber-modified epoxies. The purpose of adding rubber (a flexible element) particles to the brittle epoxy matrix is to improve the toughness, *i.e.* the ability to dissipate energy and resist catastrophic failure.

It is believed that stress whitening in these rubber-modified epoxy resins (the model adhesives) may be considered as a demonstration of the toughening mechanism imposed by the rubber particles. It is also believed that cure history controls the degree of dispersion and/or phase separation of the rubber-epoxy system[2] which, we believe, results in varying degrees of stress whitening. The variation of stress whitening, especially for the SEN tension fracture specimens, between the fully cured and undercured specimens, is most noticeable.

During our experiments, the crack tip stress whitening on the specimen surfaces perpendicular to the fracture plane was observed to occur prior to rapid crack growth for most of the cure conditions. It was observed that as the load was increased, a stress-whitened zone developed at the crack tip up to a certain extent beyond which the specimens failed rapidly. The degree to which this whitening occurred changed with the cure conditions. For example the specimens cured for long times, *i.e.* 1000 minutes and longer, at temperatures below 93°C exhibited decreasing extents of crack tip stress whitening as lower cure temperatures were used.

On the fracture surfaces, the crack tip stress-whitening zone (C.T.W.Z.) was also observed to vary with cure conditions. The cure temperature seemed to have a stronger effect on the extent of C.T.W.Z. than the cure time. The effect of carrier cloth, in general, was to increase the C.T.W.Z. It was also observed that the specimens with a higher degree of C.T.W.Z. (higher cure temperature) had rougher fracture surfaces indicating a more stable crack growth, while those exhibiting little or no C.T.W.Z. had very smooth fracture surfaces. In comparing the extreme C.T.W.Z.'s with cure, the SEN tension specimens exhibited small local whitening to full whitening in the ligament on the fracture surface.

The presence of voids in the highly-stressed regions of the adhesive seemed to affect the degree of stress whitening there. The degree of void formation in the bulk of the cured SEN tension specimens was observed to vary with the presence of the carrier cloth and the cure temperature. The presence of the carrier cloth seemed to enhance the void formation due to its constraining action on the flow of adhesive material and volatiles in the multilayered adhesive material. Furthermore, as higher cure temperatures (greater than 93°C) were used, the voids appeared to increase as observed on the fracture surfaces. Void formation seemed to enhance the crack tip whitening zones. For both adhesives, cool-down conditions did not seem to have any effect on changing the extent of void formation.

Formation of voids during the thermosetting cure process of structural adhesives has been discussed in some detail by Bikerman.[3] He maintains that the flaws form in adhesive layers of bonded joints as a result of the cure process due to a number of reasons. Some of these may be outlined in the present context as i) physical changes resulting in unfavorable stress concentrations in the form of voids due to shrinkage effects associated with curing of thermosetting adhesives; ii) physical and chemical changes resulting in weak boundary layers between the adhesive and adherend and formation of weak spots in the bulk of the adhesive film; iii) trapped air bubbles initially present at the interface of adhesive-adherend or adhesive-adhesive layers. It should be noted that some voids were also present in individual layers of the solid film prior to the final cure of the multilayered specimen.

Regarding the variations of the extent of void formation in the bulk of the model adhesives, our observations, based on the cure procedure performed in this work, indicate that cure temperature and thickness of the multilayered specimens are the strongest factors contributing to the formation of largely-voided samples. Voids initially present in the adhesive films also play a role in the extent of void formation.

THEORETICAL CONSIDERATIONS

In elastoplastic analysis of brittle epoxy adhesives a number of investigators[4,5,6] have used Irwin's concept of a plastic deformation zone at the tip of a crack to resolve the issue of stress singularity at that location. The authors believe that such a zone encompasses a stress-whitened zone. The approximate diameter of the plastic deformation zone calculated on the basis of measured Mode I strain energy release rate G_{IC}, and bulk tensile properties (tensile strength σ_y, Young's modulus E and Poisson's ratio ν) was also suggested as the optimum adhesive thickness for bonded joints.[4,5] This suggestion was offered to ensure obtaining the maximum G_{IC} value in bonded specimens as is obtained in bulk samples.

For plane strain conditions, the radius of the plastic deformation zone is calculated as[7]

$$r_{yc} = (1 - v^2)G_{IC}E/6\pi\sigma_y^2. \quad (1)$$

Equation (1) was originally used as an approximate crack length correction factor in fracture toughness measurements of high strength metallic materials. The model adhesives used in this work, however, contain large amounts of voids, varying degrees of a secondary rubbery phase and possibly some degree of anisotropy for the Metlbond 1113. Consequently, Eq. (1) may not be the best approximation to the actual plastic zone. However, due to the lack of a reasonably well-established r_{yc} expression for such non-homogeneous systems, it will be used for comparison purposes and in determination of the effects of cure conditions on fracture properties. It should be noted that even if a state of plane strain exists in the interior (*i.e.* along the thickness direction) of a SEN bulk fracture specimen a state of plane stress must exist at the specimen's free surface.[8] This is because no stresses act in the direction perpendicular to the specimen surface. Consequently, at the surface we have $\sigma_2 = \sigma_3 = 0$. For those cases where plane strain prevails, the size of the plastic zone gradually decreases from a larger (plane stress) size at the surface to a smaller (plane strain) size at the interior. The radius of the plane strain zone at the interior is theoretically predicted by Eq. (1).

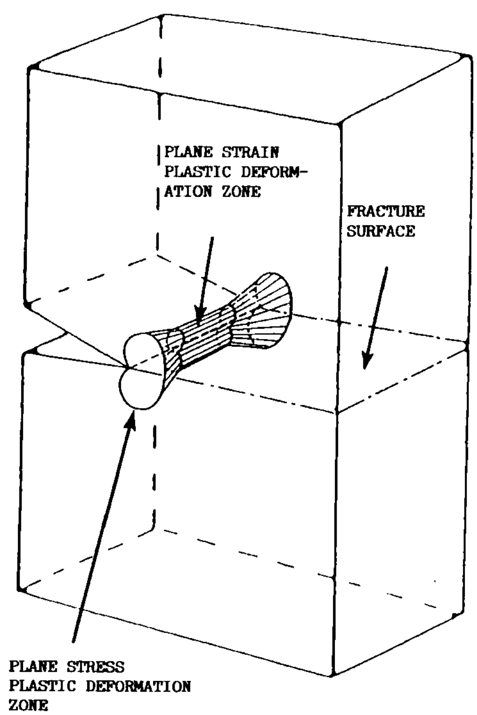

FIGURE 1 Plane stress to plane strain transition of the crack tip plastic deformation zone in plane strain single edge notched tension specimens.

Such variation in the size of the plastic deformation zone is illustrated in Figure 1. The length of the transition zone from plane stress to plane strain in the thickness direction is affected by the size of the plastic zone as given by Eq. (1). When this size is very small, yielding in the thickness direction is constrained by the surrounding unyielded material and thus the transition is very abrupt. On the other hand, if plane stress prevails in specimen interior, no transition is observed.

The exact shape of the plastic zone expected to be seen on a specimen's free surface is not a perfect circle as predicted by Irwin's small-scale-yielding assumption. A circular zone serves only as an approximation to a more complex distribution. In fact, mathematical functions describing the exact shape of crack tip plastic deformation zones are available in the literature for monolithic samples.[8,9] Furthermore, the authors believe that in Metlbond 1113 model adhesive inherent factors such as inherent voids and the carrier cloth also affect the shape of the stress-whitened zone.

In an SEN bulk fracture specimen the stress-whitened zone becomes larger at the interior of the specimen along the path of crack propagation as the crack propagates in a stable fashion. This accumulated zone will be called the Crack Tip Whitening Zone (C.T.W.Z.) and is illustrated in Figure 2. We should note that the C.T.W.Z. is distinct from the r_{yc} since it represents an accumulated value.

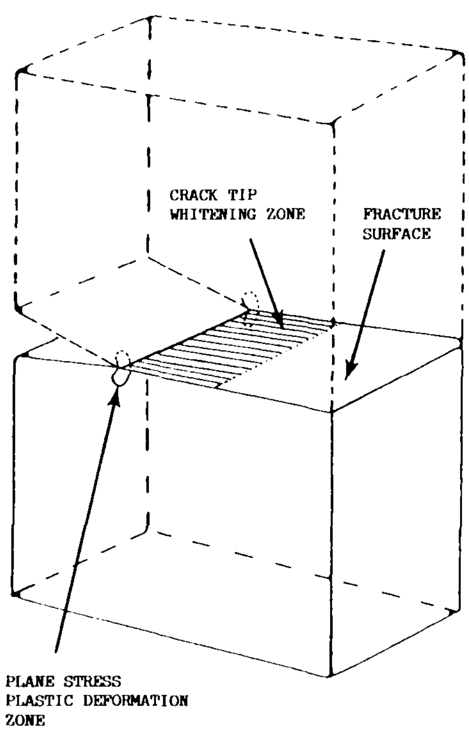

FIGURE 2 Crack tip whitening zone and its comparison with plane stress plastic deformation zone in plane strain single edge notched tension specimens.

Consequently, the size of the C.T.W.Z. is expected to be much larger than the size of of r_{yc}. The size of the C.T.W.Z. provides a measure of the total energy absorbed through irreversible processes during stable crack growth and prior to catastrophic (fast) crack propagation. Consequently, it also provides a measure of material's resistance to failure by catastrophic crack propagation.

EXPERIMENTAL PROCEDURES

Details on the preparation and testing of SEN bulk fracture specimens should be obtained from Ref. 1.

Cure schedules for bulk tensile specimens

The following abbreviated notation is used to specify the material, cure time, cure temperature and cool-down as $M_{i,j,c}$ where

M: material; A for Metlbond 1113 (with carrier cloth), B for Metlbond 1113-2 (without carrier cloth),
i: cure time (minutes) and $i = 1, \ldots, 9$, see Table I,
J: cure temperature and $J = 1, \ldots, 13$, see Table I,
c: cool-down condition; "f" for fast and "s" for slow cool-down condition.

In order to examine the fracture surfaces of the model adhesives used in this work, Scanning Electron Microscopy (SEM) was utilized. The SEM was performed using an ISI-40 microscope. Prior to SEM, the surfaces to be observed were coated with a gold sputter for 2 minutes. Paths of conduction were provided using silver paint. The SEM micrographs were taken at an angle perpendicular to the specimen surface *via* a 35 mm camera attached to the microscope.

To obtain a quantitative measure of the percentage area occupied by voids, and

TABLE I
Cure schedules and notations

Cure time (min)	Index i	Cure temperature °F(°C)	Index j
10	1	115(46)	1
20	2	140(60)	2
30	3	170(77)	3
120	4	185(85)	4
200	5	200(93)	5
500	6	215(102)	6
1,000	7	230(110)	7
5,000	8	245(118)	8
10,000	9	260(127)	9
		290(143)	10
		320(160)	11
		350(177)	12
		380(193)	13

its variation with cure conditions, photographs were taken from the failure sections of a number of bulk tensile samples using a Stereostar Zoom-T microscope (manufactured by American Optical) and a 35 mm camera attached to it. Void area measurements were manually performed by measuring the diameters of the voids, as they are normally of circular shape. These measurements were done on photographs magnified twenty times. The ratios of the void area (A_v) to the nominal area (A_T) were recorded as a measure of the percentage void area at the failure section with respect to different cure conditions. Typical values will be reported as A_v/A_T ratios.

RESULTS AND DISCUSSIONS

Void formation

Figures 3 and 4 show some typical failure sections of Metlbond 1113 and 1113-2 bulk tensile samples with different thermal cure histories. Both figures reveal that higher cure temperatures tend to result in larger void areas. Furthermore, the presence of carrier cloth results in slightly higher amounts of voids. Figures 3 and

(a)

(b)

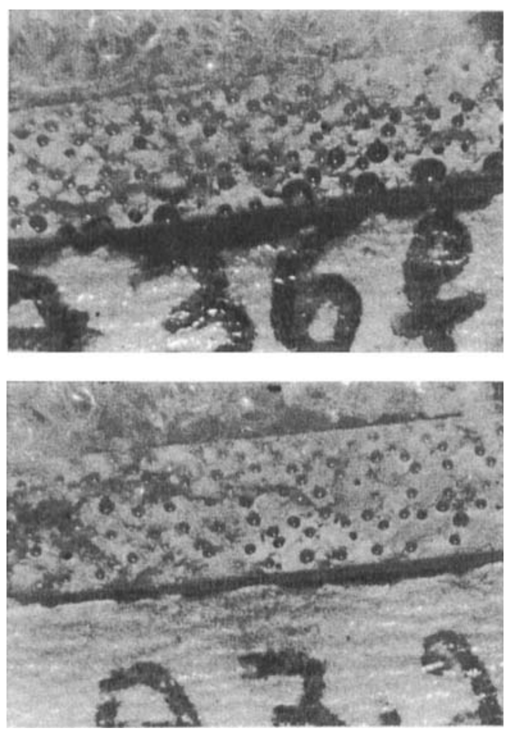

FIGURE 3 Failure sections of Metlbond 1113 bulk tensile samples showing the effects of cure schedule on void formation a) 120 min at 290°F (143°C) fast-cooled; $Av/A_T = 23.5\%$. b) 120 min at 215°F (102°C) fast-cooled; $A_v/A_T = 15\%$.

(a)

(b)

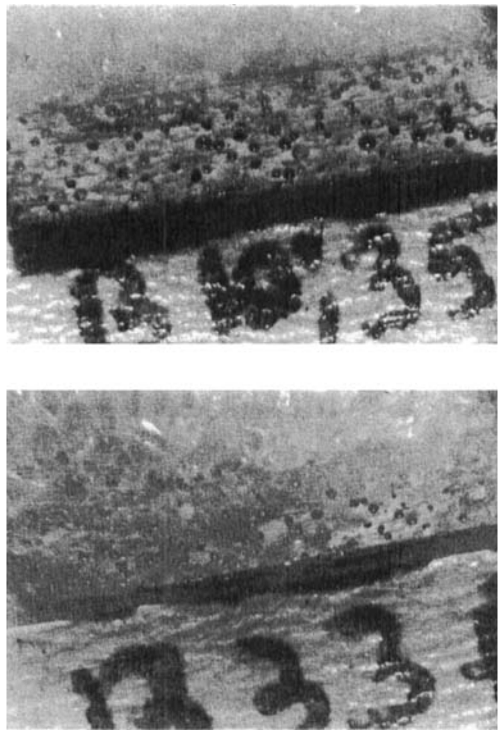

FIGURE 4 Failure sections of Metlbond 1113-2 bulk tensile sample showing the effects of cure schedule on void formation. a) 10 min at 350°F (177°C) fast-cooled; $Av/A_T = 19\%$. b) 120 min at 200°F (93°C) fast-cooled; $Av/A_T = 13\%$.

4 also reveal that the stress-whitened zones through the thickness are constrained around the voids. This shows that the presence of voids and the resulting stress concentration effects produces highly deformed regions in the bulk of the model adhesives which give rise to stress whitening. This, however, may not indicate that there would be no stress whitening if there were no voids in the bulk of the adhesives. The stress whitening, as discussed previously, is initiated at the microscopic level from the cavitation of the phase-separated rubber particles. At the macroscopic level, however, the voids, possibly, accelerate this cavitation process due to high stress concentration in the unvoided regions.

The void areas of the bulk tensile specimens were measured for a number of specimens cured at different conditions and they are tabulated in Table II as the void ratio (A_v/A_T). Also included in this table are the largest void sizes (diameters) observed on the failure sections of both adhesives.

Figure 5 shows the variation of void ratio *versus* cure temperature for the Metlbond 1113 and 1113-2 specimens with strength values falling on the optimization curves. It can be seen that for both adhesives the void ratio increases with a decreasing slope as higher cure temperatures are applied. Figure 5 also reveals that the carrier cloth seems to enhance void formation with the method of

TABLE II
Failure section void area measurements of the bulk tensile specimens

Sample	Void ratio A_v/A_t (%)	Max void dia D_{max} (mm)
A1, 11, f	20.00	1.034
A2, 8, f	17.00	0.400
A4, 6, f	15.20	0.366
A7, 4, f	12.20	0.566
A8, 3, f	9.40	0.366
A4, 4, f	0.60	0.318
A4, 5, f	12.92	0.500
A4, 9, f	19.50	0.716
A4, 10, f	23.47	0.800
B1, 12, f	19.17	0.550
B2, 9, f	16.90	0.584
B4, 7, f	14.85	0.800
B7, 5, f	12.56	0.584
B8, 3, f	9.00	0.330
B4, 5, f	12.97	0.305
B4, 9, f	17.69	0.813
B4, 10, f	17.73	0.381

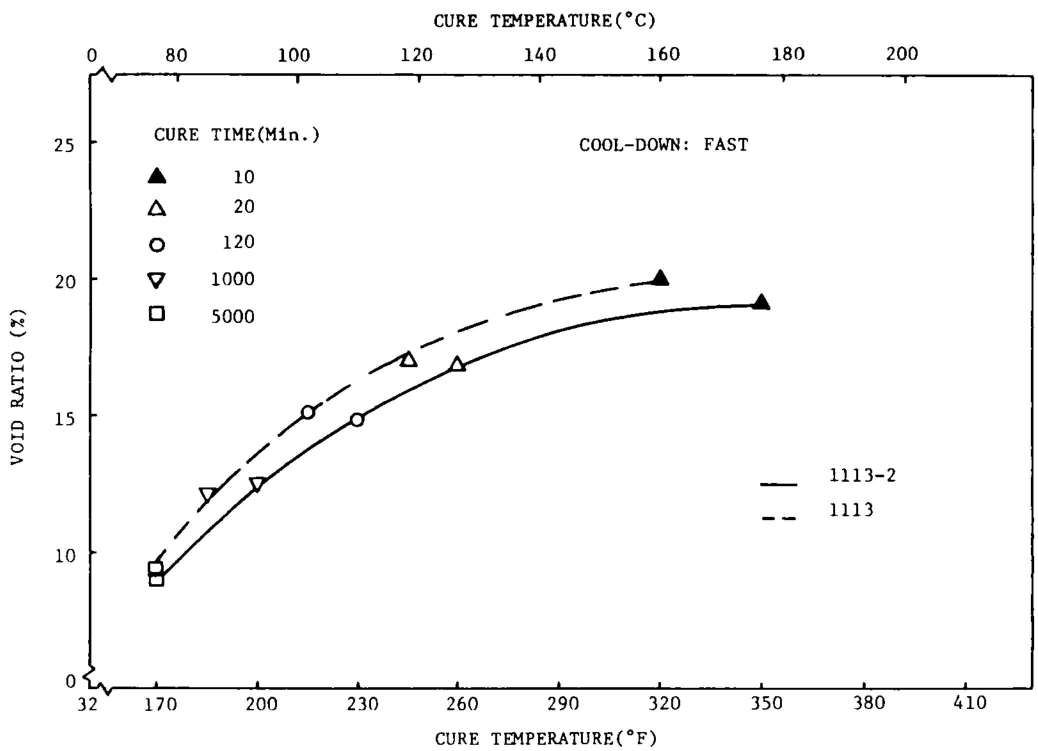

FIGURE 5 Variation of failure section void ratios for Metlbond 1113 and 1113-2 bulk tensile specimens corresponding to cure conditions giving optimum strength.

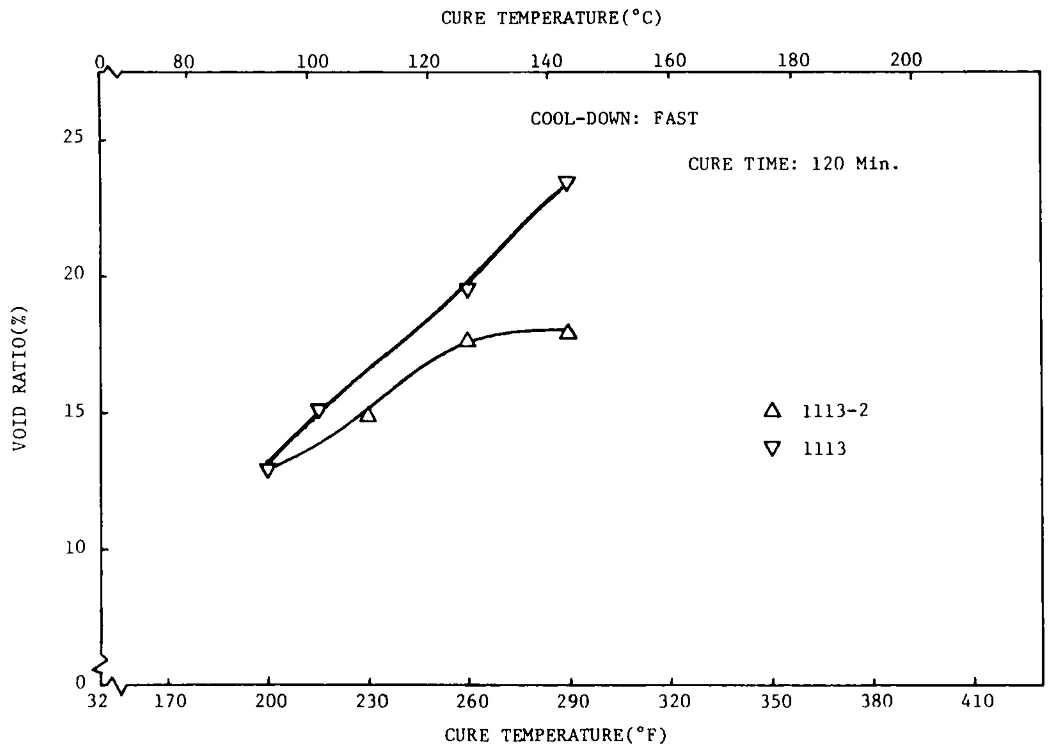

FIGURE 6 Variation of failure section void ratios for Metlbond 1113 and 1113-2 bulk tensile specimens.

curing applied in this work. This may be due to the constraints imposed by the carrier cloth (woven fibers 0.05 mm in diameter) on the flow of adhesive material and volatiles during the initial stages of the curing process within the multilayered adhesive system.

The variation of void ratio for a fixed cure time of 120 minutes and a fast cool-down condition for the model adhesives is shown in Fig. 6. It may be seen that the effect of carrier in enhancing the extent of void formation is stronger at high cure temperature than at low cure temperatures.

Measured fracture properties and C.T.W.Z.

The results from fracture testing of Metlbond 1113 and 1113-2 adhesives are summarized in Tables III and IV, respectively. All the parameters are based on average values of at least three samples. The abbreviations used in the "sample" column refer to the material, cure and cool-down conditions as shown in Table I. The other tabulated parameters are:

K_{IC}: Mode-I plane strain critical stress intensity factor;

$r_{yc} = 1/6\pi(K_{IC}/\sigma_y)^2$: plastic zone correcton factor where σ_y is the bulk tensile strength;

TABLE III
Bulk tensile fracture properties of Metlbond 1113

Sample	K_{Ic} (Mpa $- \sqrt{m}$)	r_{yc} (mm)	G_{Ic} (KJ $-$ m^{-2})	COD$_c$ (mm)	C.T.W.Z. (mm)
A4, 5, f	2.27	0.127	3.08	0.737	5.080
A4, 6, f	2.76	0.173	4.59	0.838	3.810
A4, 7, f	2.37	0.170	4.04	0.991	full*
A4, 9, f	2.19	0.173	3.57	1.070	full
A4, 10, f	2.12	0.173	3.48	0.922	full
A7, 3, f	2.46	0.142	3.52	0.584	2.540
A7, 4, f	2.89	0.178	4.18	0.584	0.762
A7, 5, f	2.76	0.188	4.81	0.762	4.450
A7, 7, f	2.51	0.190	4.60	0.991	5.080
A7, 9, f	2.09	0.157	3.29	0.914	full
A7, 10, f	1.92	0.152	2.85	0.889	full
A8, 2, f	2.81	0.203	3.79	4.111	0.585
A8, 3, f	3.04	0.188	4.62	0.635	2.540
A8, 5, f	2.78	0.173	4.59	0.790	2.540
A8, 7, f	2.31	0.145	3.48	0.864	full
A9, 2, f	3.21	0.210	4.97	0.432	1.270
A9, 5, f	3.08	0.208	5.74	0.813	4.320
A4, 6, s	2.95	0.170	4.87	0.775	4.060
A7, 4, s	3.00	0.173	4.55	0.546	1.780
A8, 3, s	3.05	0.173	4.47	0.508	0.838

* Fracture surface was completely stess-whitened.

$G_{IC} = (1 - \nu^2)K_{IC}^2/E$: Mode-I plane strain critical strain energy release rate (fracture energy);
COD$_c$: Critical crack opening displacement as measured through a C.O.D. gage at the onset of rapid crack growth;
C.T.W.Z.: crack tip whitening zone as measured on the fracture surface.

TABLE IV
Bulk tensile fracture properties of Metlbond 1113-2

Sample	K_{Ic} (Mpa $- \sqrt{m}$)	r_{yc} (mm)	G_{Ic} (KJ $-$ m^2)	COD$_c$ (mm)	C.T.W.Z. (mm)
B4, 5, f	2.26	0.135	3.31	0.762	3.302
B4, 7, f	2.45	0.142	3.83	0.864	3.810
B4, 9, f	2.19	0.145	3.22	0.960	4.570
B4, 10, f	2.17	0.145	3.32	0.889	3.560
B7, 3, f	2.16	0.122	3.03	0.470	0.635
B7, 5, f	2.57	0.145	3.69	0.589	1.270
B7, 7, f	2.37	0.173	3.42	0.914	1.780
B7, 9, f	2.33	0.183	3.82	0.787	3.810
B7, 10, f	2.26	0.178	3.80	0.660	0.584
B8, 2, f	2.34	0.150	3.45	0.394	0.584
B8, 3, f	2.62	0.147	3.73	0.432	0.711
B8, 5, f	2.46	0.140	3.45	0.483	0.686
B8, 7, f	2.47	0.165	3.80	0.787	3.302
B4, 7, s	3.29	0.213	6.75	0.754	3.050
B7, 5, s	3.39	0.221	6.62	0.483	0.584
B8, 3, s	3.43	0.224	6.55	0.414	0.508

Note that a Poisson's ratio of $v = 0.374$ is used as reported by Renieri *et al.*[10] for both Metlbond 1113 and 1113-2 in G_{IC} calculations.

Examination of Tables III and IV shows that, in general, the extent of the C.T.W.Z. increases with increasing cure temperature. The scatter in C.T.W.Z. size data, however, is more pronounced than the rest of the data reported in Tables III and IV.

Microscopic examination of the fractured samples revealed that the specimens with higher degree of C.T.W.Z. had rougher fracture surfaces, indicating more stable crack growth, while those exhibiting little or no C.T.W.Z. had very smooth fracture surface indicating fast (catastrophic) crack propagation.

One important result clearly indicated in Tables III and IV is consistently higher values for the C.T.W.Z. size for the adhesive with the carrier cloth. In other words, the adhesive with the carrier cloth (Metlbond 1113) exhibits stable (slow) crack propagation for a longer portion of the crack opening loading and, hence, has higher fracture resistance in comparison with the neat resin. This finding is corroborated by our recent fatigue test results on the same model adhesives[11] which show slower crack propagation for the adhesive with carrier cloth in comparison with the adhesive without carrier cloth. A detailed discussion on the effects of cure temperature and time on K_{IC}, r_{yc} and G_{IC} for the model adhesives is presented in Ref. 1.

Fractographic analysis

In order to observe the nature of stress whitening as seen on the surfaces of the bulk specimens, a Metlbond 1113 bulk sample (cured for 20 minutes at 177°C) was notched and loaded under tension until a partially-grown crack was developed. Further growth of the crack was stopped by unloading the sample which contained a stress-whitened zone around the tip of the partially grown crack. A piece of the sample containing part of the notch and the crack tip stress-whitened zone was carefully cut and prepared for SEM observation. Figure 7 shows the SEM micrographs illustrating the stress-whitened zone at the base of the initial notch and the tip of the arrested crack, respectively. It may be observed in Figure 7 that the stress-whitened zone contains a large number of microcracks and cavities.

Figures 8 through 11 show SEM fractographs of the fractured surfaces of Metlbond 1113 and 1113-2 bulk fracture SEN tension specimens with different cure histories. The initial crack denoted on the relevant fractographs is actually composed of a machined notch and the starter crack. Figure 8 shows the fracture surface of a Metlbond 1113 specimen with 1000-min cure at 60°C. It can be seen that a large number of microcracks exist next to the starter crack in the slow growth region. The density of these microcracks decreases towards the middle of the fracture surface where fast fracture propagation has taken place. A large number of voids (bubbles formed during the cure process) may also be observed throughout the fracture surface. A small region ahead of a starter crack tip is shown in Figure 9 with dual magnification for a Metlbond 1113 specimen cured

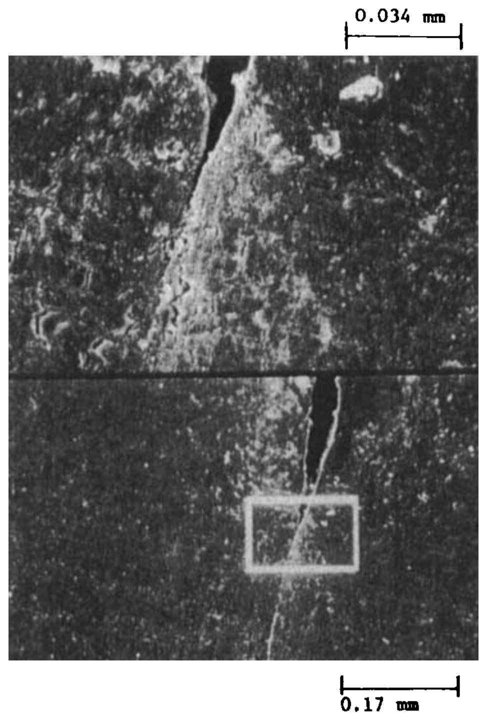

FIGURE 7 SEM dual magnification (250× and 50×) micrograph of a Metlbond 1113 specimen surface with partial fracture showing the whitened zone around the crack region (20 min cure at 177°C).

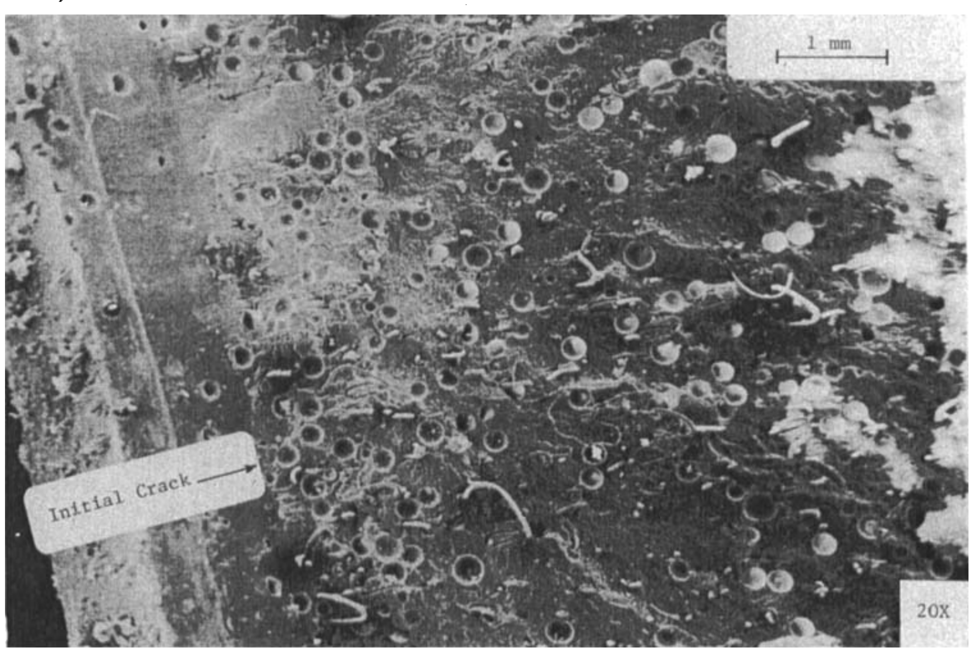

FIGURE 8 SEM fractograph of a Metlbond 1113 specimen showing the initial crack, the slow growth whitened and the fast growth regions (1000-min cure at 60°C and fast-cooled); whitened zone ~ 1.27 mm.

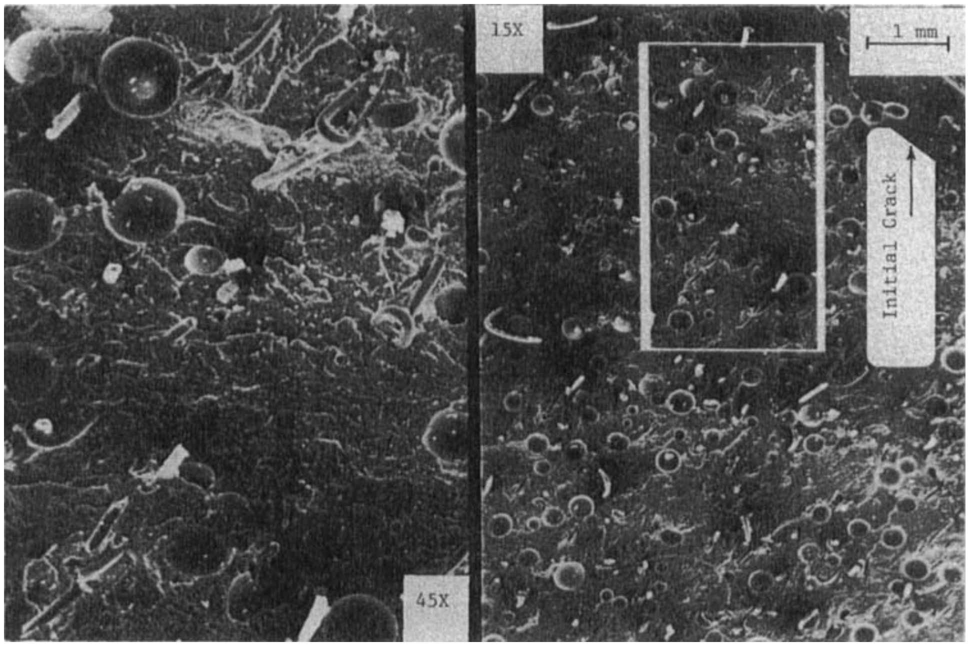

FIGURE 9 SEM dual magnification fractograph of a Metlbond 1113 specimen showing the initial crack and the slow growth whitened regions (5000-min cure at 60°C and fast-cooled).

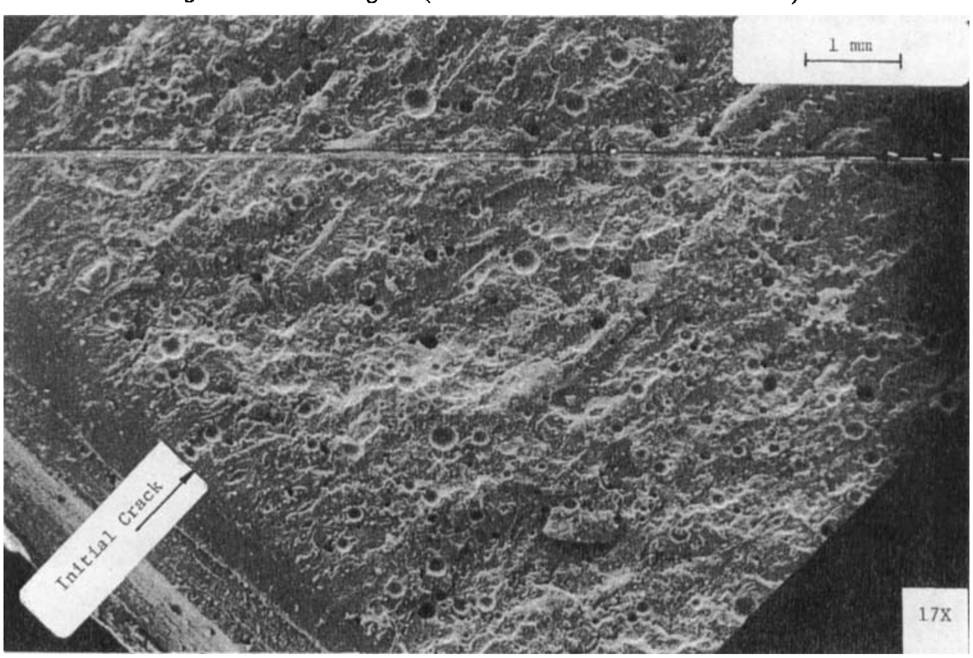

FIGURE 10 SEM fractograph of a Metlbond 1113-2 specimen showing the initial crack, the slow growth whitened and the fast growth regions (1000-min cure at 93°C and fast-cooled); whitened zone ~ 1.27 mm.

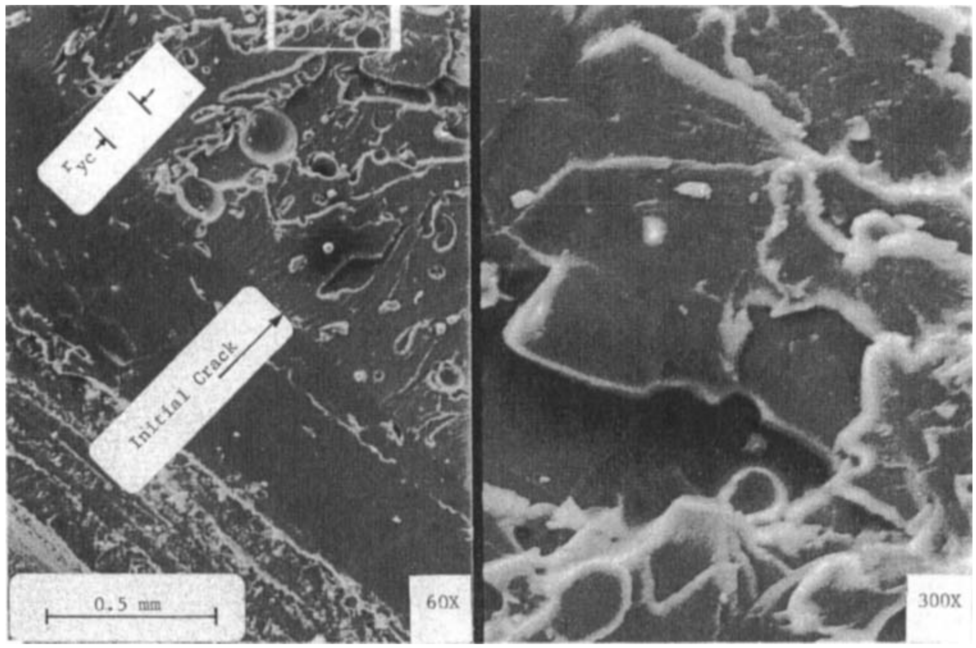

FIGURE 11 SEM dual magnification fractograph of a Metlbond 1113-2 specimen showing the initial crack tip followed by the slow growth region (1000-min, cure at 93°C and fast-cooled); $r_{yc} \sim 0.145$ mm (calculated plastic zone radius).

for 5000 minutes at 60°C. Examination of Figures 8 and 9 also indicates that the voids developed during the cure process enhance the stress whitening. This may be simply attributed to the additional stress concentration effects of the holes (voids formed during cure process) in the bulk of specimen which tend to reduce the bulk strength of the adhesive.

Figures 10 and 11 show fractographs of a Metlbond 1113-2 specimen with 10,000-minute cure at 93°C. Figure 10 shows the major portion of the fracture surface. It can be clearly observed that next to the initial crack, there is a small region with river patterns indicative of some slow growth and plastic deformation. The 60× magnification fractograph in Figure 11 also illustrates the flow pattern that is manifested as river markings. The calculated size of the plastic zone based on Eq. (1) is shown in this figure. It may be observed that this value of r_{yc} may have been an underestimate of the size of the actual plastic zone formed at the tip of the crack at fracture initiation.

Based on the SEM fractographic evidence for Metlbond 1113 and 1113-2, it seems that the presence of the carrier cloth tends to increase the extent of voids formed during cure and also enhances the stable crack growth as indicated by a generally rougher fracture surface appearance of Metlbond 1113 adhesive fracture specimens.

SUMMARY AND CONCLUSIONS

The effects of cure temperature and time on the crack tip stress-whitening behavior of model epoxy adhesives, with and without carrier cloth, were investigated by fractography. The crack tip stress-whitening zone (C.T.W.Z.) was observed to vary with cure conditions. It was also observed that formation of inherent voids prior to or during the cure process enhances the crack tip whitening zones. For this reason, experimental data revealing the effects of cure temperature and time on void formation was also presented. The C.T.W.Z., which is accumulated during stable crack propagation, provides a measure of materials resistance to failure by catastrophic crack propagation.

Experimental results revealed that in both adhesives, that is, with and without the carrier cloth, the void content increased with a decreasing slope as higher cure temperatures were applied. The presence of the carrier cloth enhanced void formation.

Another effect of the carrier cloth was observed with the crack tip whitening zones. The presence of carrier cloth resulted in larger C.T.W.Z. sizes, which indicated higher fracture resistance to catastrophic crack propagation in comparison to the neat resin. Microscopic examination revealed that stable crack growth resulted in a higher degree of C.T.W.Z. whereas catastrophic crack propagation resulted in little or no C.T.W.Z. The extent of the C.T.W.Z. was also shown to increase with increasing cure temperature.

Acknowledgments

This work was partially supported by the National Science Foundation under Grant No. GME-8007251.

References

1. H. Jozavi and E. Sancaktar, *J. Adhesion* **18,** 25 (1985).
2. J. K. Gillham, *British Polymer Journal* **17,** 2 (1985).
3. J. J. Bikerman, *The Science of Adhesive Joints* (Academic Press, New York, 1961).
4. E. Sancaktar, H. Jozavi and J. Baldwin, *Proceedings of the Southeastern XIIIth Conference on Theoretical and Applied Mechanics* (2) 752 (1986).
5. W. D. Bascom, R. L. Cottington and C. D. Timmons, *J. Appl. Polym. Sci.* **32,** 165 (1987).
6. D. L. Hunston, A. J. Kinloch, J. J. Shaw and S. S. Wang, in *Adhesive Joints,* K. L. Mittal, Ed. (Plenum Press, New York, 1984), pp. 789–807.
7. G. R. Irwin, *Proc. 7th Sagamore Conf.*, IV, pp. 63–173 (1960).
8. D. Broek, *Elementary Engineering Fracture Mechanics*, 3rd ed. (Noordhoff International Publishing, Leyden, Netherlands, 1974).
9. J. W. Dally and R. J. Sanford, *Proceedings of the 1985 SEM Spring Conference on Experimental Mechanics*, pp. 851–860.
10. M. P. Renieri, C. T. Herakovich and H. F. Brinson, *Rate and Time Dependent Behavior of Structural Adhesives*, (Virginia Polytechnic Institute Report No. VPI-E-76-7, 1976).
11. E. Sancaktar and J. Tang, *Proceedings of the 3rd International Conference on Adhesion* (Plastics and Rubber Institute, London, 1987), pp. 18–1, 18–7.
12. R. A. Pearson and A. F. Yee, *J. Maths. Sci.* **21,** 2475 (1986).